Cleaving Dihydrogen with Tetra(*o*-tolyl)diborane(4)

Nana Tsukahara,[†] Hiroki Asakawa,[†] Ka-Ho Lee,[‡] Zhenyang Lin,*[‡] Makoto Yamashita*[§¶]

[†]Department of Applied Chemistry, Faculty of Science and Engineering, Chuo University, 1-13-27, Kasuga, Bunkyo-ku, 112-8551, Tokyo, Japan.

[‡]Department of Chemistry, The Hong Kong University of Science and Technology, Clear Water Bay, Kowloon, Hong Kong

[§]Department of Applied Chemistry, Graduate School of Engineering, Nagoya University, Furo-cho, Chikusa-ku, Nagoya, Aichi 464-8603, Japan

[¶]Research Development Initiative, Chuo University, 1-13-27 Kasuga, Bunkyo-ku, Tokyo 112-8551, Japan

Supporting Information Placeholder

ABSTRACT: Tetra(*o*-tolyl)diborane(4) **1** was synthesized and characterized experimentally as well as theoretically by DFT calculations. Exposure of **1** to H_2 (1 bar) at room temperature afforded the corresponding di(*o*-tolyl)hydroborane through cleavage of the H–H and B–B bonds. DFT calculations suggested a diarylborylanion character for the transition state.

Since the discovery of heterogeneously catalyzed hydrogenations by Sabatier,[1] catalytic and stoichiometric hydrogenations with H_2 have represented major research fields in molecular transition-metal chemistry.[2] However, the limited availability of precious metals, which are active as hydrogenation catalysts, has fueled the quest for more sustainable options. Two such recently developed alternatives are: i) the replacement of the precious metals with base metals, and ii) the use of catalysts based on main-group elements.[3] The latter can be subdivided into two classes: i) frustrated Lewis pairs (FLPs),[4] which can cleave H_2 heterolytically, and ii) main-group element compounds in low oxidation states. The latter class involves group 13 or 14 elements such as C(II), Si(II), Ge(I), Sn(I), P(II), B(0), B(II), Al(I), and Ga(I).[5] Our recent report regarding the deprotonation of H_2 with boryllithium[6] is also relevant in this context, as boryl anions can be considered as a B(I) species. As far as reactive trivalent group 13 compounds are concerned, the reaction of an antiaromatic borole with H_2,[7] the reversible cleavage of H_2 with dianionic diboraanthracenes,[8] and FLP-like reactivity of diaminogallium with cooperation of ligand[9] have been recently reported.

Recently, we reported the synthesis of the unsymmetrical diborane(4) pinB–BMes$_2$[10] and its reactivity toward CO and *tert*-butylisocyanide.[10a] This diborane(4) reacts also with alkynes to form diborylalkenes[10b] and the regioselectivity of the diboration to afford *syn*- or *anti*-diborylalkenes can be controlled by addition of a catalytic amount of base and 1,2-dimethoxyethane. This diborane(4) furthermore reacts with 2,6-dimethylphenylisocyanide to furnish an 1,2-oxaboretane ring through a ring-contraction of Bpin.[10c] This characteristic reactivity of pinB–BMes$_2$ was attributed to the high electron affinity arising from the two parallely arranged vacant p-orbitals on the two boron atoms.[10d] Similarly high electron affinity was reported for Mes$_2$B–B(Mes)Ph, which was synthesized from (MeO)$_2$B–B(OMe)$_2$ and is capable to form the corresponding radical anion and dianion.[11] Moreover, Mes$_2$B–B(Mes)Ph represents the only reported example of a tetraaryldiborane(4). Herein, we report the synthesis of tetra(*o*-tolyl)diborane(4) **1** and its reactivity toward H_2 at room temperature, as well as a mechanistic study based on DFT calculations.

By careful choice of the precursor, **1** could be obtained in 30% isolated yield from the reaction between B$_2$cat$_2$ and *o*-tolMgBr (Scheme 1). The molecular structure of **1** was determined by single-crystal X-ray diffraction analysis (Figure 1). In the crystal, **1** adopts an almost orthogonally twisted structure [C8–B1–B2–C15 = 101.9(7)°], similar to that of Mes$_2$B–B(Mes)Ph.[11a] The ^{1}H NMR spectrum of **1** exhibited four magnetically equivalent *o*-tol groups at room temperature, indicating free rotation around the B–B and B–C bonds on the NMR timescale. The ^{11}B NMR spectrum of **1** in C$_6$D$_6$ showed a broad signal at 89 ppm. Dissolution of **1** in THF did not alter the [11]B

NMR chemical shift, indicating that THF does not coordinate to the boron atom in **1**.

Scheme 1. Synthesis of tetra(o-tolyl)diborane(4) **1**.
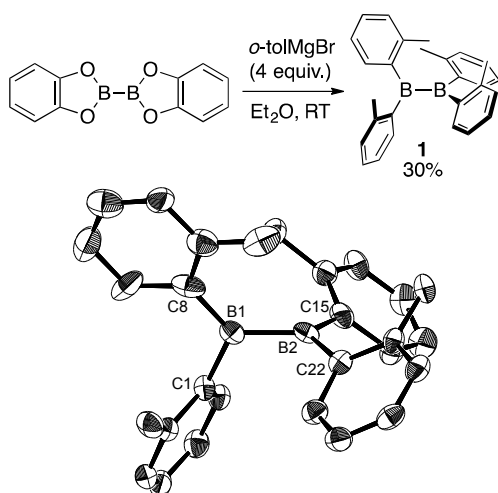

Figure 1. Molecular structure of **1** (thermal ellipsoids set at 50% probability; one of two independent molecules and hydrogen atoms were omitted for clarity).

To estimate the electron affinity of **1**, electrochemical measurements and DFT calculations were conducted. The cyclic voltammogram of a THF solution of **1** showed a reversible reduction wave at −2.1 V (vs. Cp_2Fe/Cp_2Fe^+). The first reduction potential of **1** is thus less negative than that of previously reported pinB-BMes$_2$ (−2.5 V vs. Cp_2Fe/Cp_2Fe^+). Similar to our previous report,[10d] we also calculated the dependency of the LUMO level and the free energy of **1** on the torsion angle C(*ipso*)–B–B–C(*ipso*). The optimized structure of **1** contains a torsion angle of −96.6°, which is comparable to the crystal structure and leads to a calculated LUMO level of −1.29 eV. Increasing the torsion angle of **1** from −90° to 0° in increments of 10° lowers the LUMO energy (as well as the stability) as shown in Figure 2. When the torsion angle approaches 0°, the LUMO energy drops to −2.20 eV and the corresponding structure is destabilized by 8.51 kcal/mol. This relatively mild destabilization suggests that rotation around the B–B bond should occur at room temperature. The lowering of the LUMO of **1** upon rotation around the B–B bond should be attributed to the overlap of the two vacant p-orbitals on the two boron centers (Figure 3). The LUMO of **1** in the ground state (−96.6°) consists of π*-orbitals of two o-tol rings and one vacant p-orbital of the boron atom. The LUMO+1 is of similar energy and mainly localized on the other B(o-tol)$_2$ moiety, while the LUMO of **1** (0.0) exhibits two completely merged vacant p-orbitals on the two boron atoms. It should be noted that the HOMOs of
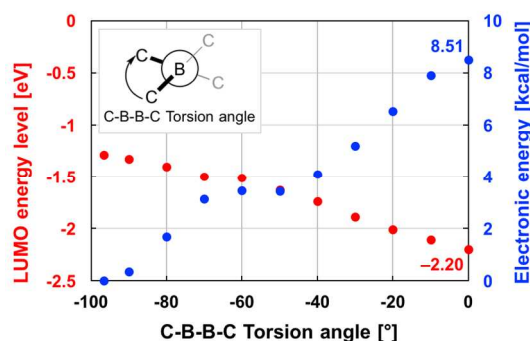
both rotational isomers exhibit a B–B σ-bond character.

Figure 2. Dependency of the LUMO energy level (in eV) and the relative stability (in kcal/mol) of **1** on the torsion angle of the C(*ipso*)–B–B–C(*ipso*) moiety.
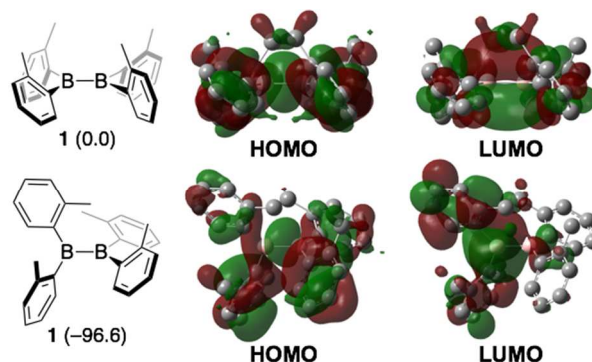

Figure 3. Frontier orbitals of the rotational isomers of **1** at C(*ipso*)–B–B–C(*ipso*) = 0.0° (top) and C(*ipso*)–B–B–C(*ipso*) = −96.6° (bottom).

Tetra(o-tolyl)diborane(4) **1** reacts directly with H_2. Exposing a hexane solution of **1** for 2 h to H_2 (1 bar) at room temperature afforded di(o-tolyl)hydroborane **2** in 52% yield (Scheme 2). The crystal structure of **2** revealed a dimeric structure with hydride bridges (Figure 4, left), which is similar to those of previously reported dimeric diarylhydroboranes.[12] The solid state IR spectrum of **2** exhibited a characteristic μ-H vibration at 1520 cm^{-1}, which is comparable to that of $[HB(C_6F_5)_2]_2$.[12b] Dissolution of **2** in C_6D_6 or $CDCl_3$ led to five B-bonded ^{1}H nuclei and three ^{11}B nuclei in the ^{1}H{^{11}B} and ^{11}B NMR spectra, respectively. This behavior should be attributed to a monomer/dimer equilibrium[13] and a potential coordination of solvent molecules to the highly Lewis acidic boron center of the monomer.[12b,14] In contrast, dissolution of **2** in THF led to a simple NMR spectra indicating a formation of **2**·THF. Addition of pyridine to isolated **2** without solvent at room temperature afforded single crystals of the corresponding pyridine-hydroborane complex **3**, which was completely characterized by

NMR spectroscopy, X-ray analysis, and high-resolution FAB mass spectroscopy.

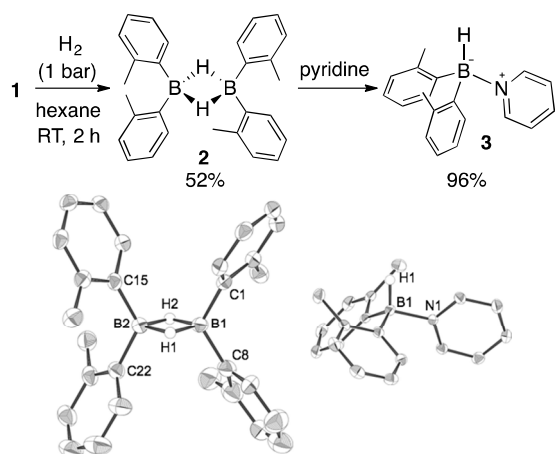**Scheme 2.** Reaction of **1** with H$_2$

Figure 4. Molecular structures of **2** (left) and **3** (right) (thermal ellipsoids at 50% probability; hydrogen atoms except for B–H were omitted for clarity).

To get a better understanding of the detailed pathway for the reaction of **1** with H$_2$, DFT calculations were performed (Scheme 3). The results suggested that the overall reaction should consist of four steps. The hydrogenation of the B–B bond in **1** should be initiated by coordination of the H–H bond to one of the vacant p-orbitals of one of the boron atom to afford intermediate **4**, in which the C(*ipso*)–B–B–C(*ipso*) torsion angle changed to −55.1°, indicating that the strong electron affinity of **1** enables the binding to H$_2$. Upon coordination of H$_2$, both the H–H and B–B bonds should elongate and the coordination geometry of the H$_2$-coordinated boron atom should become pyramidalized. Subsequently, cleavage of the B–B σ-bond should be accompanied by a proton-migrating H–H bond cleavage via **TS$_{4-5}$**, leading to the formation of the dimeric hydroborane intermediate **5**, which contains a hydride and an o-tolyl group as bridging ligands. Here, it should be noted that in **TS$_{4-5}$**, the *ipso* carbon atom of one o-tolyl group starts to interact with the boron atom it is not directly attached to [C(ipso)–B 2.347 Å]. **TS$_{4-5}$** represents the rate-determining step of the reaction sequence and requires an overall activation free energy of 19.8 kcal/mol. The resulting intermediate (**5**) is thus located 8.3 kcal/mol below the reference point (**1** + H$_2$). Intermediate **5** involves a characteristic B–C–B three-center-two-electron bond, which has recently been confirmed by Wagner.[15] Dissociation of **5** to afford monomeric hydroborane **6**, and the subsequent dimerization of **6** to afford hydride-bridged dimer **2** through the two low-energy transition states **TS$_{5-6}$** and **TS$_{6-2}$** include relatively low activation bar-

riers. The overall reaction from **1** + H$_2$ to give **5** is exergonic by 20.1 kcal/mol.

Scheme 3. Proposed reaction mechanism and energy profile for the hydrogenolysis of **1** [Ar = o-tolyl; calculated at M06/6-31G(d) level of theory with solvent effect of benzene(SMD); dashed lines correspond to the formation/cleavage of bonds or 3-center-2-electron bonds].[a]
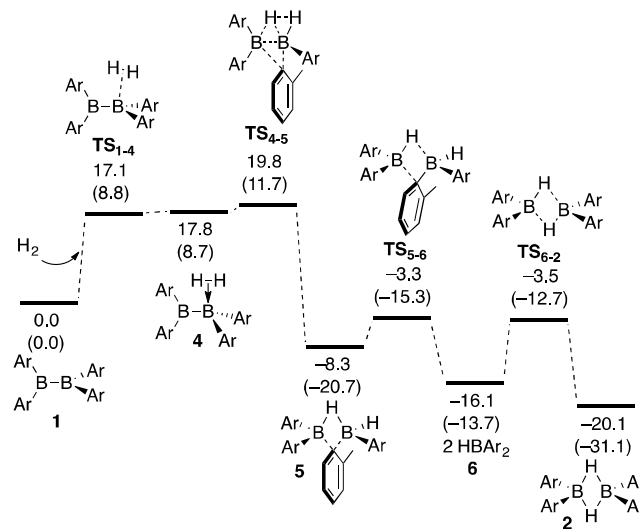
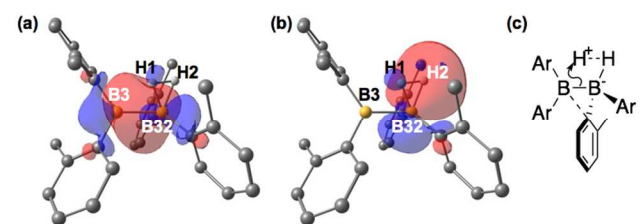[a]Relative free energies and electronic energies (in parentheses) are given in kcal/mol.

Figure 5. Selected natural bond orbitals: (a) NBO91 and (b) NBO92 of **TS$_{4-5}$**, as well as (c) schematic illustration of the diarylborylanion character of B3 in **TS$_{4-5}$** (numbering of atoms is based on the calculations)

To characterize the transition state for the H–H bond cleavage, an NBO analysis was performed. The calculated natural charge on the migrating hydrogen atom (H1: +0.306) is more positive than that on the other hydrogen atom (H2: +0.200), indicating that H1 should be transferred as a proton. The NBO analysis on **TS$_{4-5}$** showed that the vacant orbital of the migrating proton H1 interacts with both the bonding orbitals of the H–B and B–B bonds (NBO 91 and NBO92 shown in Figure 5a,b), and exhibits significant second-order perturbation energies (E$_2$) of 352.52 and 200.49 kcal/mol, respectively. Thus, the transition states cleaving H–H bond (**TS$_{4-5}$**) may be described as an intramolecular deprotonation by an "sp^2-sp^3 diborane" that exhibits a diarylborylanion

character (Figure 5c). The proton-migrating charac-
ter of **TS$_{4-5}$** is similar to that of the deprotonation of
H$_2$ with boryllithium,[6] and to that for the cleavage of
H–H by an antiaromatic borole involving a B–C bond
cleavage.[7]

In conclusion, tetra(*o*-tolyl)diborane(4) **1** was syn-
thesized, and characterized experimentally as well as
theoretically by DFT calculations. Exposure of **1** to H$_2$
at room temperature afforded the corresponding dia-
rylhydroborane via cleavage of the H–H and B–B
bonds. DFT calculations suggested a diarylborylan-
ion character for the transition state.

ASSOCIATED CONTENT

Supporting Information

The Supporting Information is available free of charge
on the ACS Publications website at DOI: 10.1021/jacs.x.

Experimental and computational details (PDF)
Crystallographic data (CIF)
DFT Coordinates (XYZ)

AUTHOR INFORMATION

Corresponding Authors

*makoto@oec.apchem.nagoya-u.ac.jp, *chzlin@ust.hk

Notes

The authors declare no competing financial interests.

ACKNOWLEDGMENT

REFERENCES

(1) Sabatier, P., *Ind. Eng. Chem.* **1926,** *18*, 1005-1008.

(2) (a) *The handbook of homogeneous hydrogenation*. Wiley-
VCH: 2007; (b) Hartwig, J. F., Chapter 7, Oxidative addition. In
Organotransition Metal Chemistry: From Bonding to Catalysis,
University Science Books: Sausalito, CA, 2010.

(3) (a) Power, P. P., *Nature* **2010,** *463*, 171-177; (b) Power, P. P.,
Acc. Chem. Res. **2011,** *44*, 627-637; (c) Martin, D.; Soleilhavoup,
M.; Bertrand, G., *Chem. Sci.* **2011,** *2*, 389-399.

(4) (a) Stephan, D. W., *Chem. Commun.* **2010,** *46*, 8526-8533;
(b) Welch, G. C.; Juan, R. R. S.; Masuda, J. D.; Stephan, D. W.,
Science **2006,** *314*, 1124-1126; (c) Chase, P. A.; Welch, G. C.; Jurca,
T.; Stephan, D. W., *Angew. Chem. Int. Ed.* **2007,** *46*, 8050-8053;
(d) Stephan, D. W.; Erker, G., *Angew. Chem. Int. Ed.* **2010,** *49*, 46-
76; (e) Stephan, D. W., *Org. Biomol. Chem.* **2012,** *10*, 5740-5746;
(f) Hounjet, L. J.; Stephan, D. W., *Org. Process Res. Dev.* **2014,** *18*,
385-391; (g) Stephan, D. W., *Acc. Chem. Res.* **2015,** *48*, 306-316;
(h) Stephan, D. W., *J. Am. Chem. Soc.* **2015,** *137*, 10018-10032; (i)
Stephan, D. W.; Erker, G., *Angew. Chem. Int. Ed.* **2015,** *54*, 6400-

6441; (j) Weicker, S. A.; Stephan, D. W., *Bull. Chem. Soc. Jpn.*
2015, *88*, 1003-1016.

(5) (a) Spikes, G. H.; Fettinger, J. C.; Power, P. P., *J. Am. Chem.
Soc.* **2005,** *127*, 12232-12233; (b) Frey, G. D.; Lavallo, V.;
Donnadieu, B.; Schoeller, W. W.; Bertrand, G., *Science* **2007,** *316*,
439-441; (c) Peng, Y.; Brynda, M.; Ellis, B. D.; Fettinger, J. C.;
Rivard, E.; Power, P. P., *Chem. Commun.* **2008**, 6042-6044; (d)
Zhu, Z.; Wang, X.; Peng, Y.; Lei, H.; Fettinger, J. C.; Rivard, E.;
Power, P. P., *Angew. Chem. Int. Ed.* **2009,** *48*, 2031-2034; (e)
Seifert, A.; Scheid, D.; Linti, G.; Zessin, T., *Chem. Eur. J.* **2009,** *15*,
12114-12120; (f) Shoji, Y.; Matsuo, T.; Hashizume, D.; Fueno, H.;
Tanaka, K.; Tamao, K., *J. Am. Chem. Soc.* **2010,** *132*, 8258-8260;
(g) Li, J.; Schenk, C.; Goedecke, C.; Frenking, G.; Jones, C., *J. Am.
Chem. Soc.* **2011,** *133*, 18622-18625; (h) Protchenko, A. V.;
Birjkumar, K. H.; Dange, D.; Schwarz, A. D.; Vidovic, D.; Jones,
C.; Kaltsoyannis, N.; Mountford, P.; Aldridge, S., *J. Am. Chem.
Soc.* **2012,** *134*, 6500-6503; (i) Schäfer, A.; Reißmann, M.; Schäfer,
A.; Schmidtmann, M.; Müller, T., *Chem. Eur. J.* **2014,** *20*, 9381-
9386; (j) Hadlington, T. J.; Jones, C., *Chem. Commun.* **2014,** *50*,
2321-2323; (k) Vasko, P.; Wang, S.; Tuononen, H. M.; Power, P.
P., *Angew. Chem. Int. Ed.* **2015,** *54*, 3802-3805; (l) Arrowsmith, M.;
Böhnke, J.; Braunschweig, H.; Celik, M. A.; Dellermann, T.;
Hammond, K., *Chem. Eur. J.* **2016,** *22*, 17169-17172; (m) Nagata, K.;
Murosaki, T.; Agou, T.; Sasamori, T.; Matsuo, T.; Tokitoh, N.,
Angew. Chem. Int. Ed. **2016,** *55*, 12877-12880; (n) Hinz, A.; Schulz,
A.; Villinger, A., *Angew. Chem. Int. Ed.* **2016,** *55*, 12214-12218.

(6) Dettenrieder, N.; Aramaki, Y.; Wolf, B. M.; Maichle-
Mössmer, C.; Zhao, X.; Yamashita, M.; Nozaki, K.; Anwander, R.,
Angew. Chem. Int. Ed. **2014,** *53*, 6259-6262.

(7) (a) Fan, C.; Mercier, L. G.; Piers, W. E.; Tuononen, H. M.;
Parvez, M., *J. Am. Chem. Soc.* **2010,** *132*, 9604-9606; (b)
Houghton, A. Y.; Karttunen, V. A.; Fan, C.; Piers, W. E.;
Tuononen, H. M., *J. Am. Chem. Soc.* **2013,** *135*, 941-947.

(8) von Grotthuss, E.; Diefenbach, M.; Bolte, M.; Lerner, H.-
W.; Holthausen, M. C.; Wagner, M., *Angew. Chem. Int. Ed.* **2016,**
55, 14067-14071.

(9) Abdalla, J. A. B.; Riddlestone, I. M.; Tirfoin, R.; Aldridge, S.,
Angew. Chem. Int. Ed. **2015,** *54*, 5098-5102.

(10) (a) Asakawa, H.; Lee, K.-H.; Lin, Z.; Yamashita, M., *Nat.
Commun.* **2014,** *5*, 4245; (b) Kojima, C.; Lee, K.-H.; Lin, Z.;
Yamashita, M., *J. Am. Chem. Soc.* **2016,** *138*, 6662-6669; (c)
Katsuma, Y.; Asakawa, H.; Lee, K.-H.; Lin, Z.; Yamashita, M.,
Organometallics **2016,** *35*, 2563-2566; (d) Asakawa, H.; Lee, K.-H.;
Furukawa, K.; Lin, Z.; Yamashita, M., *Chem. Eur. J.* **2015,** *21*, 4267-
4271.

(11) (a) Moezzi, A.; Olmstead, M. M.; Bartlett, R. A.; Power, P.
P., *Organometallics* **1992,** *11*, 2383-2388; (b) Moezzi, A.;
Olmstead, M. M.; Power, P. P., *J. Am. Chem. Soc.* **1992,** *114*, 2715-
2717; (c) Power, P. P., *Inorg. Chim. Acta* **1992,** *198–200*, 443-447.

(12) (a) Entwistle, C. D.; Marder, T. B.; Smith, P. S.; Howard, J.
A. K.; Fox, M. A.; Mason, S. A., *J. Organomet. Chem.* **2003,** *680*,
165-172; (b) Parks, D. J.; Piers, W. E.; Yap, G. P. A.,
Organometallics **1998,** *17*, 5492-5503; (c) Hübner, A.; Qu, Z.-W.;
Englert, U.; Bolte, M.; Lerner, H.-W.; Holthausen, M. C.;
Wagner, M., *J. Am. Chem. Soc.* **2011,** *133*, 4596-4609; (d) Seven,
Ö.; Qu, Z.-W.; Zhu, H.; Bolte, M.; Lerner, H.-W.; Holthausen, M.
C.; Wagner, M., *Chem. Eur. J.* **2012,** *18*, 11284-11295.

(13) The possible involvement of trimer and tetramer in the
equilibrium was also examined by DFT calculations. However,
stable structures could not be obtained for these compounds.
For details, see Supporting Information.

(14) The coordination of B(C$_6$F$_5$)$_3$ to toluene in the gas phase
was calculated to be thermoneutral; see: Timoshkin, A. Y.;
Frenking, G., *Organometallics* **2008,** *27*, 371-380.

(15) Hübner, A.; Diefenbach, M.; Bolte, M.; Lerner, H.-W.;
Holthausen, M. C.; Wagner, M., *Angew. Chem. Int. Ed.* **2012,** *51*,
12514-12518.

Authors are required to submit a graphic entry for the Table of Contents (TOC) that, in conjunction with the man-uscript title, should give the reader a representative idea of one of the following: A key structure, reaction, equation, concept, or theorem, etc., that is discussed in the manuscript. Consult the journal's Instructions for Authors for TOC graphic specifications.

deprotonating TS with diarylborylanion character